February 4, 1997

MASSACHUSETTS INSTITUTE OF TECHNOLOGY
Physics Department

8.13 - 8.14 Spring 1997

Junior Laboratory Experiment #13

Mössbauer Spectroscopy

This experiment is an exploration of ultra high-resolution spectroscopy by means of recoilless emission and absorption of gamma rays - the Mössbauer Effect.

PREPARATORY QUESTIONS

1. Derive an exact relativistic expression for the recoil energy of the nucleus of mass M that emits a gamma ray of energy E, and evaluate it for an iron nucleus and $E = 14.4$ keV.
2. Suppose the above atom is embedded in an iron crystallite which has a mass of 10^{-6} grams and is free to move. Compute the recoil energy of the crystal. If the emission of the gamma ray is "recoilless", i.e. the nucleus does not acquire momentum relative to the center of mass of the crystal, what would be the energy shift of the gamma ray photon due to the recoil of the crystal?
3. Draw an energy level diagram of the ^{57}Fe nucleus in a magnetic field and show the transitions which give rise to the Zeeman pattern you expect to see in this experiment.
4. Why is the multiplicity of energy levels of a nucleus due to electric quadrupole interaction with an electric field gradient acting alone (quadrupole splitting) less than the multiplicity of levels due to magnetic dipole interaction with a magnetic field (Zeeman splitting)?
5. How fast must the source be moved relative to the absorber to shift the frequency of resonant absorption by the natural line width?
6. Why can't you do this experiment with the 6.4 keV photons also emitted by the source?

QUANTITIES YOU CAN MEASURE

1. Natural width of the 14.4 keV Mössbauer line of ^{57}Fe.
2. Ratio of the magnetic moments of the ^{57}Fe nucleus in its ground and first excited states.
3. Magnetic field at the iron nuclei in metallic iron and in Fe_2O_3.
4. Quadrupole splitting of the first excited state of the ^{57}Fe nucleus in the bivalent and trivalent state of the iron atom.
5. Relative isomer shifts of the 14.4 keV line in metallic iron, steel and compounds of iron.
6. Effect of relativistic time dilatation (second-order Doppler shift) on the frequency of the 14.4 keV line through measurement of the temperature coefficient.

INTRODUCTION

The resolution of a spectrum measurement is characterized by the ratio $E/\Delta E$, where E is the energy of the spectrum line and ΔE is a measure of the line width , e.g. the full width at half maximum. The NaI scintillation spectrometer in the Compton experiment produces a spectrum of 662 keV gamma rays with a resolution of about 10. At the same energy the spectrum obtained with the germanium solid state cryogenic detector in the X-ray Physics experiment has a resolution of 200. The echelle spectrograms used in the solar and the hydrogenic atoms experiments for measurements in the visible portion of the spectrum have resolutions of the order of 5×10^4.

Imagine spectroscopy with a resolution of 10^{12}! Recoilless emission and resonance absorption of gamma radiation by nuclei, discovered by Rudolf Mössbauer in 1957, makes possible such ultra high-resolution spectroscopy in the gamma-ray region of the spectrum. Mössbauer spectroscopy has been used in many areas of physics and chemistry, for example in the determination of life-times of excited nuclear states, in the measurement of nuclear magnetic moments, in the study of electric and magnetic fields in atoms and crystals, and in the testing of special relativity and the equivalence principle. The phenomenon itself is also of great interest. In this experiment you will observe the Mössbauer effect and explore several of its applications in ultra-high resolution spectroscopy.

Mössbauer himself provided a particularly lucid introduction to the physics and application of recoilless gamma-ray emission and absorption in his 1961 Nobel Lecture which is available in the Junior Lab library shelf. More technical discussions are found in the texts of Melissinos (1966) and Gasiorowicz (1974). "The Mössbauer Effect" by Hans Frauenfelder (1962) contains historical and theoretical background and reprints of articles bearing on all the topics in this set of experiments. Excerpts from Frauenfelder's book are available on the Junior Lab reference shelves.

You will use as the source of recoilless gamma rays a commercial "Mössbauer" source consisting of ^{57}Co diffused into a platinum substrate. The ^{57}Co nucleus decays by K-electron capture to an excited state of ^{57}Fe according to the scheme shown in Figure 1. The newly created iron atom settles down in the crystal lattice of the substrate and the d-shell vacancies in its electronic structure are filled in such a way as to eliminate the magnetic field at the nucleus. 91% of the excited iron nuclei decay by gamma-ray emission to the first excited state ($3/2^-$). The latter has a comparatively long half-life of 9.8×10^{-8} seconds and decays to the ground state with the emission of 14.4 keV gamma rays of which a substantial fraction are emitted without recoil or Doppler broadening. The natural line width of the 14.4 keV line is $\Gamma = h \ln 2/2\pi\tau_{1/2} = 4.7 \times 10^{-9}$ eV, corresponding to a fractional width of $\sim 3 \times 10^{-13}$. In the absence of a field the magnetic substates of the excited and ground states are degenerate. Under this condition the spectrum of gamma rays from the recoilless emissions appears as a single ultra-narrow line on top of a Doppler-broadened and recoil-shifted "normal" emission line, as illustrated in Figure 2a.

In a similar way, absorbers containing ^{57}Fe can have ultra-narrow recoilless resonance absorption lines on top of a normal Doppler-broadened and recoil-shifted 14.4 keV line. Mössbauer absorption lines may be shifted slightly in energy with respect to the emission line by virtue of the different electronic environments of the nuclei in the source and the absorber (the "chemical" shift), and they may be split by the interactions between the nuclear magnetic dipole and/or electric quadrupole moments with internal or external fields in the absorber (Zeeman or electric quadrupole splittings). In a famous experiment that tested the red shift predicted by the general theory of relativity, the shift was caused by a ~100-foot difference in height of the source and absorber!

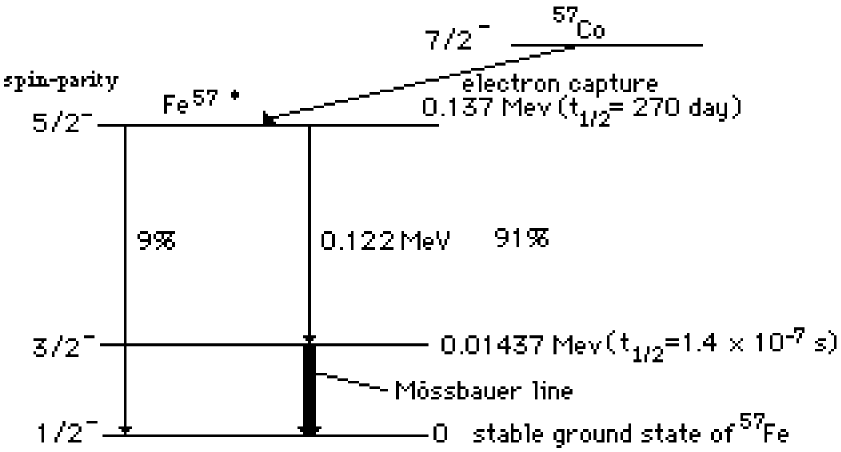

Figure 1. Decay scheme of ^{57}Co. The 14.4-keV transition 3/2 --> 1/2 is the one used in many Mössbauer experiments. (Frauenfelder 1962, p. 50).

Figure 2b is a schematic representation of the absorption cross section of $^{57}\mathrm{Fe}^{++}$ in an ionic compound in which the iron nuclei are in a nonuniform electric field which produces an electric quadrupole splitting $\Delta\varepsilon$ in addition to an isomer shift $\delta\varepsilon$ (see below). The measurement process in Mössbauer spectroscopy uses the Doppler shift produced by controlled motion of the source to scan the emission line back and forth in energy over the absorption spectrum of a sample containing the same isotope in its ground state and in a particular chemical or physical environment of interest. The advantage of using a source with a single emission line for performing such a scan is apparent from a consideration of the complications that occur if a multi-line source is used to scan the absorption spectrum of a multi-line absorber.

A primary objective of this experiment is to determine the width of the convolved recoilless emission and absorption lines of the 14.4 keV transition in ^{57}Fe. The velocity width Γ_v

corresponding to a given energy width Γ is given by the simple formula

$$\Gamma_v = c\,(\Gamma/E_o),$$

where E_o is the mean energy (14.4 keV) of the gamma rays in the line, and c is the speed of light. The velocity width corresponding to the natural line width estimated above is 0.1 mm s^{-1}. Clearly, one will require a velocity resolution at least an order of magnitude smaller to obtain a useful profile of the line shape.

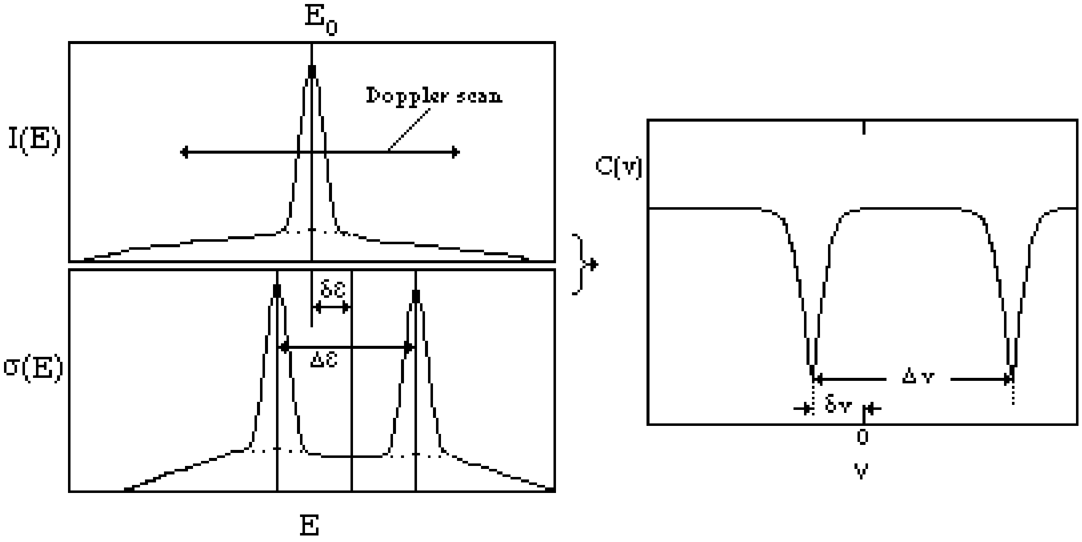

(a) (b)

Figure 2. (a) Schematic plots against energy, E, of (top) the intensity, $I(E)$, of gamma rays from a single line Mössbauer source moving with velocity v relative to a Mössbauer absorber, and (bottom) absorption cross section $\sigma(E)$ of the absorber. (b) Schematic plot of counting rate $C(V)$ of a detector exposed to the gamma rays after they have traversed the absorber against velocity V. In (a) the energy separation of the two absorption lines is $\Delta\varepsilon$, and the Doppler shift due to the motion of the source is $\delta\varepsilon$. In (b) the velocity separation of the two lines is $\Delta V= c\,(\Delta\varepsilon /E_o)$, where E_o is approximately the average energy of the two lines.

Suppose that the recoilless photons are emitted with a distribution in energy, $I(E)$, centered around E_o. When the source moves at a velocity V *toward* the absorber, a photon emitted with energy E in the rest frame of the source has an energy

$$E'=E(1+V/c) \tag{1}$$

in the rest frame of the absorber. (By convention, positive velocity indicates the source moving toward the absorber.) Call $\sigma(E)$ the cross-section for absorption by the absorber atoms of photons of energy E, and call η the effective area of the detector which we assume to be constant over the narrow energy range of the 14.4 keV line. Then the counting rate when the emitter is moving with velocity V *will* be

$$C(V) = \eta \int_0^\infty dE\, I(E) \exp\left[-\frac{\sigma(E')Nx}{A}\right] , \qquad (2)$$

where x is the thickness of the absorber in g cm^{-2}, A is the atomic weight, and N is Avagadro's number. We assume that both the emission line intensity and the absorption cross section have the Lorentzian form, i.e.

$$I(E) = \frac{I_0\,(\Gamma/2)^2}{(E-E_0)^2 + (\Gamma/2)^2} , \qquad (3)$$

and

$$\sigma(E) = \frac{\sigma_0\,(\Gamma/2)^2}{(E-E_0-\Delta E)^2 + (\Gamma/2)^2} . \qquad (4)$$

where ΔE is the intrinsic shift of the resonance energy in the absorber relative to the source due to chemical or other effects, and I_0 and σ_0 are the values at the line centers. The counting rate of a detector placed in the beam of gamma rays after the beam has traversed the absorber is then

$$C(V) = \eta I_0 \int_0^\infty dE\, \frac{(\Gamma/2)^2}{(E-E_0)^2 + (\Gamma/2)^2} \exp\left[-\frac{\sigma_0\,(\Gamma/2)^2}{(E\,[1+V/c\,] - E_0 - \Delta E\,)^2 + (\Gamma/2)^2}\,\frac{Nx}{A}\right]. \qquad (5$$

For thin absorbers $\sigma_0 Nx/A \ll 1$, and one can obtain an approximate expression for the line profile by expanding the exponential factor in (5) and keeping only the first two terms. The integral can then be evaluated by contour integration in the complex plane to obtain

$$C(V) = C_0\left[\,1 - \frac{B}{(E_0\,V/c - \Delta E\,)^2 + \Gamma^2}\right] , \qquad (6)$$

where C_0 is a constant that depends on the strength of the source and the thickness of the absorber and B is a constant that depends only on the thickness of the source. This function has a minimum at $V=(\Delta E/E_0)c$ and a full width at half maximum (FWHM) of $2c\Gamma/E_0$.

For thick absorbers one must resort to numerical integration of equation (4). Figure 3 shows the line profiles for various thicknesses of absorber corresponding to values of $\alpha = \sigma_0 Nx/A$ ranging from 0.1 to 10. The width of the absorption line at half amplitude clearly increases with increasing absorber thickness in the range of thickness where nearly all the recoilless emission is absorbed near the line center, i.e. in the range of "line saturation". One can correct for this saturation effect by measuring the line breadth as a function of absorber thickness and extrapolating to zero thickness. (Note that in an actual observation the non-recoilless emission causes a background counting rate that does not vary with velocity but does decrease with increasing thickness of the absorber.)

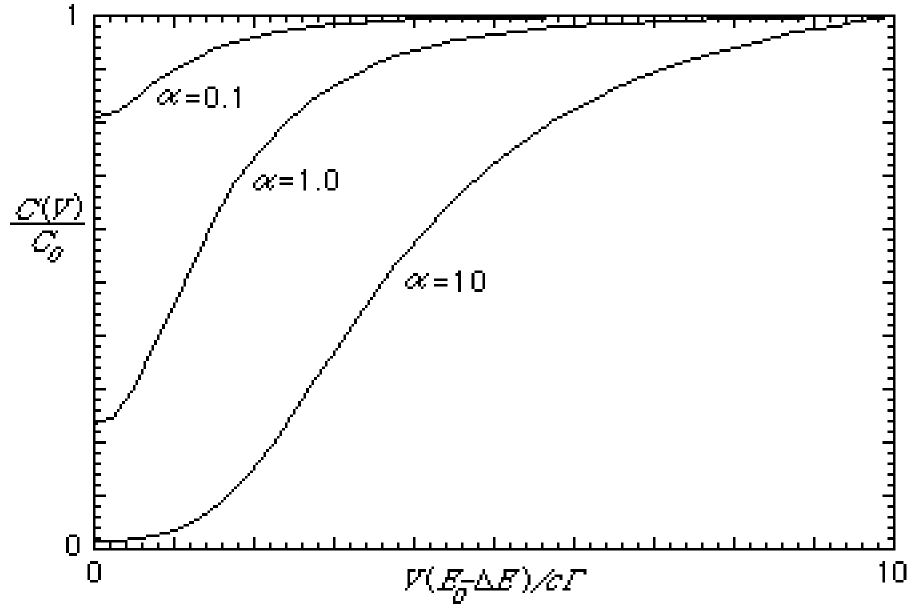

Figure 3. Calculated shapes of recoilless gamma-ray absorption lines for various thicknesses of absorber. The normalized counting rates are plotted as functions of velocity expressed in units of $c\Gamma/(E_0-\Delta E) \approx c\Gamma/E_0$..

Many interesting effects can be observed in absorption spectra; several are discussed below. Zeeman splitting in an internal magnetic field. The nucleus of an iron atom in metallic iron and certain iron compounds is in an intense magnetic field produced primarily by unpaired electrons of the same atom. Since both the nuclear states involved in the 14.4 keV transition have spin and associated magnetic moments, both are split by the interactions between the nuclear magnetic moment and the magnetic field of the electrons. In an isolated atom the effect of this interaction on optical transitions is characterized as hyperfine splitting. When the atom is bound in a crystal lattice the orientation of the internal magnetic field due to the electrons is fixed with respect to the lattice. As a result, the effect of the electronic magnetic field on the energy of the nucleus may be thought of and analyzed simply as the Zeeman effect in a new context. The number of absorption peaks and their separations depend on the angular momenta and associated magnetic moments of the absorber nucleus in each state. A measurement of the internal Zeeman splitting can be combined with knowledge of the magnetic moment of the ground state (which can be derived from other experiments) to deduce the magnetic field at the iron nucleus in the absorber, and the magnetic moment of the first excited state.

Isomer shift. If the chemical environment of the iron nuclei in the source and absorber are different then the electron densities will, in general, be different. Since the electromagnetic interaction between the electrons and the nucleus depends (though only slightly) on the electron density at the nucleus and on the nuclear radius, and since the radius of the iron nucleus changes slightly in the 14.4 keV transition, there is, in general, a shift of the resonance energy from source to absorber if the host materials are different. This is called the "isomer shift" because the excited states of nuclei were originally called isomers. The magnitude of the shift depends on the s-electron density at the nucleus. If there is greater electron density at the absorbing nucleus than at the emitting nucleus, additional energy must be given to the gamma-ray by moving the source toward the absorber. There are differences on the order of a factor of ten between the isomeric shifts of Fe in the +2 and+3 ionization states in the lattice, and these differences may easily be measured. An isomer shift in a Zeeman or quadrupole pattern appears as a shift of the "center of gravity" of the lines.

Electric quadrupole splitting. The nucleus may be in an electric field with a gradient due to nearby ions with unfilled atomic levels. If the nucleus has a quadrupole (or higher) electric moment, i.e. if its electric charge distribution is not spherically symmetric, its energy levels will be split by amounts that depend on the projections of its spin in the direction of the field gradient. The ground state is shifted by the quadrupole interaction, and the first excited level is split into two levels: thus two transitions with energies $\Delta E_2 \pm 1/2\ \Delta E_3$, are possible, yielding two absorption peaks, as shown in Figure 2.

Anisotropic emission by polarized nuclei. Each of the possible transitions that give rise to the Zeeman spectrum of lines of an absorber with ^{57}Fe nuclei in a strong internal magnetic field has a particular anisotropic radiation pattern relative to the direction of the field. The orientation of the internal field of a ferromagnetic material can be controlled by a much weaker external field. Thus changes in the relative intensities of the lines in the Zeeman pattern can be caused by placing the absorber in the field of a strong permanent magnet. Figure 4 shows the expected intensities of the Zeeman absorption lines in an absorber with no preferred orientation (unmagnetized) and in an absorber magnetized in a direction perpendicular to the direction of propagation.

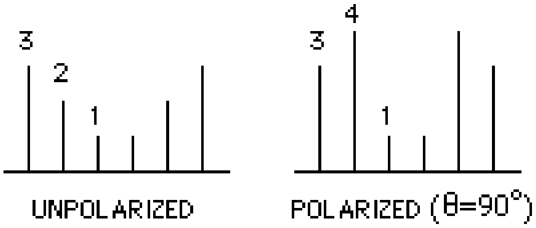

Figure 4. Expected relative intensities of the Zeeman pattern of ^{57}Fe for an unpolarized absorber and for an absorber polarized perpendicular to the direction of propagation. (from Hanna *et al.* 1960).

Effect of relativistic time dilatation (second-order Doppler shift) on the frequency of the 14.4 keV line through measurement of the temperature coefficient. Vibration frequencies of atoms in a crystal at room temperature are of the order of 10^{13} Hertz. Therefore, a ^{57}Fe nucleus in its first excited state makes many oscillations before it decays and, is whizzing around with a mean square velocity of $\sim kT/m$ during this time. According to the special theory of relativity, a clock aboard the moving nucleus runs slow relative to one at rest in the laboratory by the fraction

$$(1/\gamma) = (1 - V^2/c^2)^{1/2}. \qquad (7)$$

Thus the center energy of a Mössbauer line emitted from a source at temperature T is shifted down in energy by an amount of the order $\langle (V/c)^2 \rangle E = (kT/mc^2)E$, where E is the unshifted energy. The center energy of an absorption line is similarly shifted. This effect was discovered in the gravitational red-shift experiment by Pound and Rebke (1960). They had to take special care in their experiment to maintain the source and absorber at the same temperature within a fraction of a degree so that the temperature shifts did not mask the gravitational red shift. The temperature effect provides a clear demonstration of the so-called "twin paradox" of special relativity and resolves any doubt as to whether the accelerations involved in return trips negate the dilation of time suffered by clocks in motion. The exact theory of the effect can be found in the collection of reprints contained in the book of Frauenfelder (1962).

APPARATUS

Figure 5 is a schematic diagram of the set up. A proportional gas counter (see Melissinos, p 181) and associated measurement chain are used to detect selectively the ~14.4 keV photons emitted by excited ^{57}Fe nuclei produced by the beta decay of ^{57}Co in a specially prepared "Mössbauer" source (i.e. ^{57}Co diffused into a platinum substrate). Some of the ~14.4 keV photons are emitted by nuclei that share the recoil momentum with macroscopic bits of the matter in which they are imbedded ("recoiless emission") with the result that their fractional spread in energy, or line width, $\Delta E/E$, is extraordinarily narrow, of the order of 10^{-13}. A sample containing ^{57}Fe atoms in an environment that permits recoiless absorption of 14.4 keV photons, is placed between the source and the proportional counter. The source is mounted on a piston which moves back and forth with a velocity that is a periodic sawtooth function of time. This motion causes a corresponding sawtooth Doppler shift in the energies of the photons that traverse the sample. In effect, the narrow emission line is swept back and forth in energy over the recoilless absorption lines of the ^{57}Fe in the absorber. Meanwhile, an MCA, operated in its "multiscaling" mode, is triggered at the start of each velocity cycle to count clock pulses in a scaler. When a 14.4 keV photon, having traversed the absorber, triggers the proportional counter, the resulting pulse is counted in the memory channel of the MCA with the address given by the current number in the clock scaler. Thus, after a given exposure, each channel of the MCA contains a number of counts proportional to the number of photons that traversed the absorber within the narrow range of energies corresponding to the narrow range of velocities of the piston during which the clock scaler dwelled on the address of that channel. The contents of each count register are displayed on the screen of the MCA. In the absence of a Mössbauer absorption line the average number of counts in the various velocity intervals will be equal within the Poisson statistics of counting. If there is a Mössbauer absorption line at an energy equal to the Doppler-shifted energy at

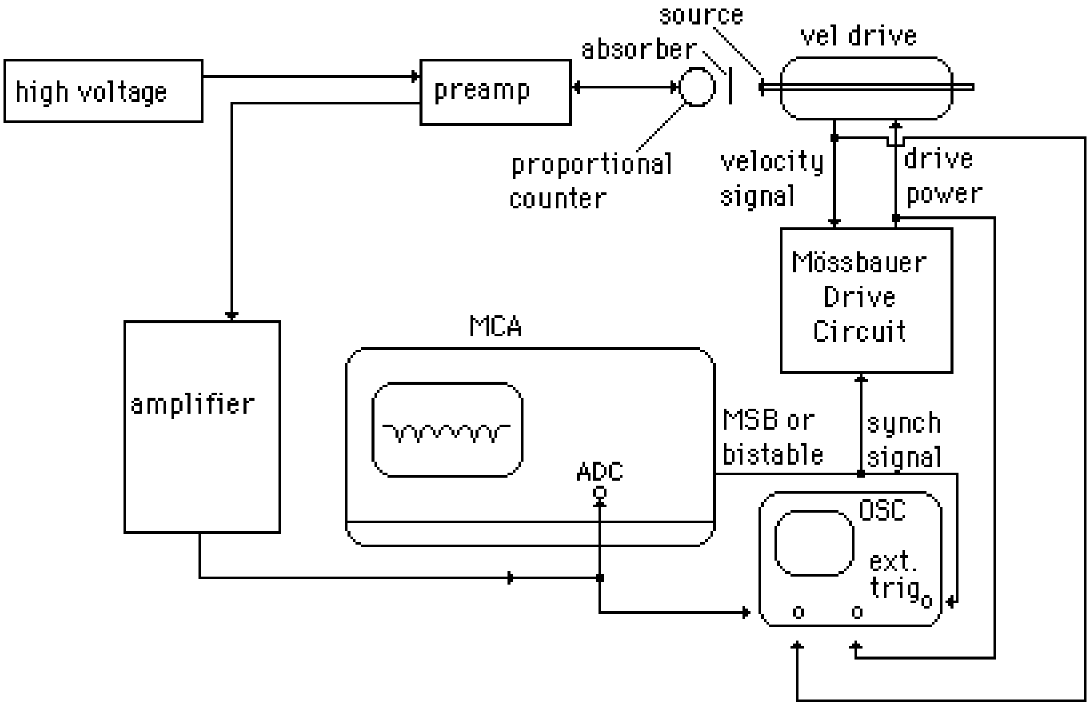

Figure 5. Arrangement of the Austin apparatus for Mössbauer spectroscopy.

some particular velocity, then the counting rate during the time that pulses are addressed to that velocity channel will be reduced, and the accumulated deficiency of counts in that and neighboring channels will be seen as an "absorption line" on the MCA screen.

Detailed instructions for operation of the drive circuit are in a binder located near the equipment.

The piston on which the source is mounted is driven by the magnetic force produced by a drive current in the coil of the transducer. The resulting motion generates in a sense coil an induced current that is proportional to the velocity. The sense current is compared to a reference linear current ramp, and the difference (error) signal is fed back to the drive-current amplifier in such a manner as to reduce the difference between the sense current and the reference current. In this way the velocity of the piston is kept accurately proportional to the reference current. In the mode of operation used in these experiments, the reference current is a sawtooth function of time with a slow, linear rise from $-I_0$ to $+I_0$ with a rapid flyback to $-I_0$. The corresponding velocity of the piston is therefore also a sawtooth function of time with a slow, linear rise from $-V_0$ to $+V_0$and a rapid flyback.

The signal at MSB (most significant bit of the channel address scaler) of the MCA is used to trigger an independent ramp generator in the velocity drive circuit. The circuit is designed for a nominal trigger rate of 6Hz; it functions satisfactorily at ~5Hz which is the closest rate that can be obtained from the MCA with the thumb wheels set at 2,2 (200 µs per channel). It is essential that this setting be used. The thumb wheel on the Austin drive adjusts the amplitude of the motion, and hence, with the fixed frequency, the amplitude of the velocity sweep (the rotary switch just below the thumb wheel is not used). The gain in the servo feedback loop, controlled by the "fidelity" pot, should be adjusted to achieve a linear velocity ramp. If you hear a sound emanating from the drive motor, the gain is way too high. Display the drive and velocity signals on the two channels of the dual beam oscilloscope and check that 1) the velocity ramp is linear and 2) the drive signal has an <u>average</u> value near zero and is not in high frequency oscillation.

Caution #1: The motor switch on the electronic drive generator should be ON only when the MCA is in the MCSR collect mode so the motors are receiving proper ramp voltages. The reason is that when the MCA is in the non-collect mode it produces rapid pulses which can cause the motors to heat up to the point where the insulation of the coil windings breaks down and a short circuit occurs.)

CAUTION #2: Do not touch the fragile window on the counter.

CAUTION #3: Before switching the high-voltage power supply of the proportional counter on or off, or when making a change in the HV setting, be sure to have the HV/OPERATE switch in the HV position. Failure to follow this procedure may

damage the delicate field effect transistor in the input stage of the preamplifier by inducing a voltage surge across it.

When everything is properly set up, the distribution of pulses fed to the ADC should appear on the oscilloscope approximately as shown in Figure 6. The pulses should be positive, and those identified as due to the 14.4 keV Mossbauer line should have amplitudes near 5 volts.

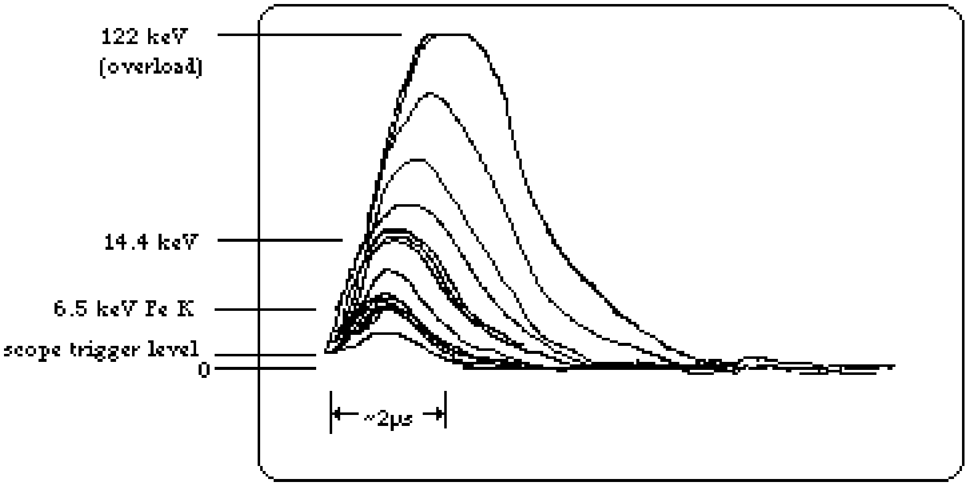

Figure 6. Approximate appearance on the oscilloscope of the distribution of pulses fed to the ADC of the MCA when everything is properly set.

The following is a start-up Check List:

1. Check the connections. Put the HV/OPERATE switch on the preamplifier in the HV position.
2. Turn on the power switch of the electronics rack (leave the Mössbauer drive switch in <u>OFF</u> position).
3. Turn on the MCA.
4. Turn on the high voltage supply, and raise the voltage to ~1800 v.
5. Turn the HV/OPER switch to OPER.
6. Examine the output pulses from the amplifier with the oscilloscope and adjust the gain controls so that the pulses in the strong 6.4 keV iron K-line have an amplitude of about 2.5 volts. Identify the fainter 14.4 keV Mössbauer line at about twice the amplitude of the iron K-line.
7. With the MCA in PHA mode record the spectrum of pulses and identify the peaks due to the 6.5 and 14.4 keV photons.

8. Adjust the lower and upper level discriminators of the MCA so that only pulses in the 14.4 keV peak are accepted.

9. Change the MCA mode to multiscaling (MSC). Set the time per channel control (thumb wheels) to 200 µs per channel (to give a sweep repetition rate of ~ 5 Hz). Start the sweep.

10. Adjust the thumb wheels on the Mössbauer drive to 80. Turn on the drive and verify that it is moving the piston back and forth at the frequency (~5 Hz) of the MCA sweep. Check the drive and velocity signals.

11. Place the enriched ^{57}Fe iron foil absorber in the absorber mount.

12. Clear the MCA momentarily, start recording, and watch the Mossbauer spectrum of the Zeeman-split 14.4 keV line build up on the MCA screen.

EXPERIMENTS

1. Zeeman splitting of the ground and first excited states of ^{57}Fe in an iron foil.

The primary purpose of this part of the experiment is to record and understand the Zeeman splitting of the 14.4 keV gamma-ray line emitted by ^{57}Fe nuclei in an iron foil. The other purpose is to establish a convenient secondary calibration standard.

Record the absorption spectrum for a sufficient time to obtain at least several thousand counts per channel so that you can measure accurate centroid values, intensities, and shapes of the six lines of the pattern. Using the cursors, measure the channel positions of each of the absorption peaks in the MCA display. You can transfer the MCA data to your own diskette (from the Physics Supply room) and plot the spectra on the IBM PC. Detailed directions for the data transfer are provided nearby.

Next, without changing any of the settings, carry out an absolute calibration of the drive motion with the interferometer, as described below. Derive from your measured spectrum and the velocity calibration data the separation in velocity (mm/s) between adjacent pairs of lines in the six-line Zeeman pattern. With these results in hand you can use the quickly observable Zeeman pattern of the enriched iron foil as a secondary calibration standard for each of your subsequent Mössbauer spectrum measurements.

Convert the velocity separations between the lines of the Zeeman pattern into energy separations. The magnetic moment of the ground state of ^{57}Fe has been measured by electron spin resonance techniques to be +0.0903±0.0007 nuclear magnetons. Using this fact, and interpreting the Zeeman pattern in terms of the energy level diagram (see Melissinos, p. 277), determine the internal magnetic field at a nucleus of iron in the iron foil absorber, and the magnetic moment of the first excited state. Discuss the experimental errors in the values you have obtained. With the data in hand can you verify the discovery of Hanna *et al.* (1960) that the magnetic moments of the ground and first excited states have opposite signs?

2. Absolute calibration

Calibration of the velocity sweep is accomplished with the aid of a Michelson interferometer shown schematically in Figure 7. A beam of coherent light from a laser is split by partial reflection from a glass slide so that the two parts traverse different paths before striking the same spot on a photodiode. While the length of one path is fixed, the length of the other path varies because it includes a reflection from a mirror mounted on the moving piston. When the piston moves a distance equal to one-half of the wavelength of the laser light, the length of the path increases by one wave length, the phase of the beam at the photodiode changes by 360°, and the intensity of the recombined beam at the photodiode goes through one cycle of constructive and destructive interference. Every cycle of interference produces one cycle of a sinusoidal voltage signal from the photodiode that can be registered as one pulse by the MCA. The rate of pulses is $2V/\lambda$. If we call T the time interval during which pulses are directed to a given channel by the clock register, i. e., the dwell time per channel, N the number of sweeps made during the course of a calibration run, and C the number of counts recorded in the given channel, then the mean velocity corresponding to that channel is

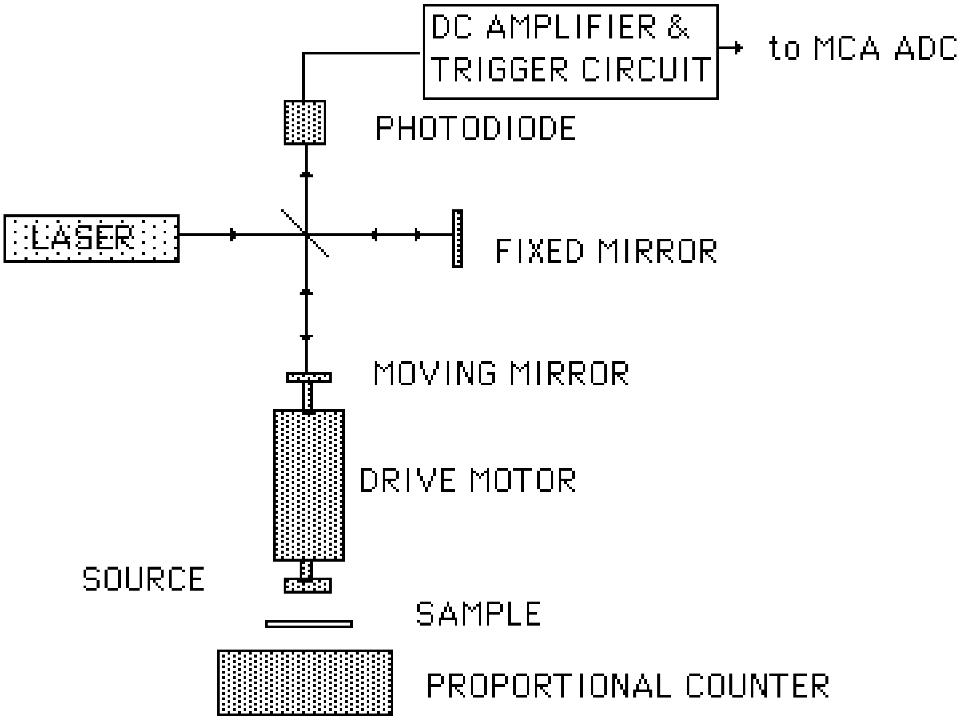

Figure 7. Schematic diagram of the Michelson interferometer for calibration of the velocity sweep.

$$V = \frac{C\lambda}{2NT} \ . \tag{8}$$

A special amplifier and trigger circuit is provided to receive the frequency-modulated sunusoid signal from the photodiode and generate a logic pulse for every cycle of the signal. When the circuit is properly adjusted, each logic pulse will be counted in the MCA channel corresponding to the velocity of the piston at the moment of its occurence, and the pattern on the screen will take on an appearance like that shown in Figure 8. The operation of the system is a little tricky, so you may have to fuss patiently with the adjustments to get it going reliably.

Run the Mössbauer setup with an enriched iron foil absorber to obtain the 6-line Zeeman pattern that will be your secondary calibrator. Record the channel numbers of the absorption line centroids. Without changing any of the setting of the Mössbauer drive circuit except to turn it off and on, procede with the calibration as follows:

*Connect the Wavetek sine wave generator directly to the input of the special circuit. Connect the bistable most-significant-bit (MSB) output from the rear panel of the MCA to the Mössbauer drive circuit, to the external trigger input of the oscilloscope, and to a Timer/Scaler to count the triggers that control the Mössbauer drive.

*Examine the amplifier output of the special circuit with the oscilloscope, and check the performance of the amplifier over the range of frequencies you expect in the signals from the interferometer.

*Examine the logic pulse simultaneously with the amplifier signal, and adjust the threshhold and pulse-width controls to obtain reliable production of logic pulses over the range of expected frequencies.

*Turn on the MCA in the repeating multiscaling mode (toggle switch on lower panel at MSCR). Leave the Mössbauer driver turned off.

*Synchronize the oscilloscope sweep with the MCA sweep, by triggering the oscilloscope externally with the same MSB signal from the rear of the MCA.

*Set the frequency of the sine wave generator to 10.00 kHz, and feed the logic pulses from the special circuit to the MCA ADC. Adjust the discriminators to achieve reliable counting. Run the MCA for 1000 sweeps. Record the total number of counts in 1000 channels by using the cursors and the integrate feature of the MCA (see the Omega MCA manual). Compute the effective dwell time per channel for the system receiving 10^4 counts per second. Repeat the test at 10^2, 10^3, 10^5 Hz to verify correct operation over the range of pulse rates that you may encounter..

*Turn on the laser and adjust the orientation of the beam splitter and the adjustable mirror to bring the split beams together on the photodiode.

*Connect the photodiode to the input of the special circuit.

*Turn on the MCA sweep.

*Examine the amplifier output and watch for the interference signal as you make fine adjustments of the mirrors to maximize the amplitude of the frequency-modulated sinusoid.

*Examine the pulse output and verify reliable pulse production over the entire velocity range.

*Feed the pulses to the MCA ADC. Run for a sufficient number of sweeps to obtain a smooth pattern like that illustrated in Figure 8.

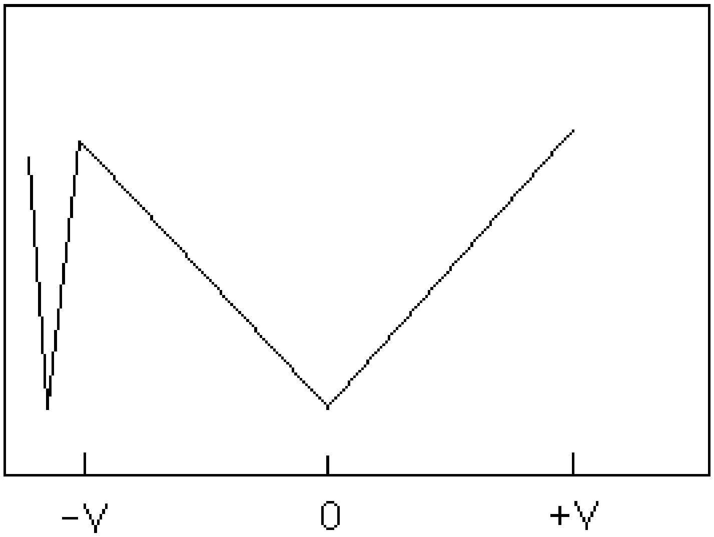

Figure 8. Appearance of the MCA screen after several minutes of operation with the interferomter velocity calibrator. The sharp feature at the start is produced during the rapid reversal of the velocity of the piston at the high speed end of its stroke.

Suppose you record N=1000 sweeps and find C=2000 counts in a particular channel. With the MCA thumb-wheel sweep controls set at 2,2, you may have found int the Wavetek calibration that T=0.000170 sec. The wavelength of the HeNe laser light is λ=6328 Å, or 6.328x10^{-5} cm. According to equation (8), the piston velocity at that part of the cycle is

$$V=6.238*10^{-5}*2000/1000/.000170/2=0.367 \text{ cm/s.}$$

The following is a menu of possible investigations:

a. Properties of the Resonant Line Shape.

In this experiment, you will use an absorber of sodium ferrocyanide ($Na_3Fe(CN)_6\ 10H_2O$) which has no magnetic field or electric field gradient at the crystal sites of the iron nuclei. Absorbers of three different thicknesses are available. This allows you to measure the line width as a function of thickness so that you can extrapolate your results to zero thickness.

Derive a value for the intrinsic width of the 14.4 keV first excited state of ^{57}Fe and compute the implied lifetime of the excited state. What other causes of line broadening may be present in your data?

b. Temperature coefficient of the Mössbauer lines and the twin "paradox".

The temperature effect is a shift in the resonant frequency of an absorption line due to the second order Doppler effect which amounts to a slowing of the atomic "clocks" in a heated sample due to their thermal motion relative to the reference atomic clocks in the lab. According to the theory of relativity, the effect should be of the order of $(v/c)^2 \sim kT/mc^2 \sim 10^{-13}$. That is small indeed, but accessible to Mössbauer spectroscopy. It is also a proof that the so-called "twin paradox" (not really a paradox since it follows logically from the theory of relativity) is really true, i.e. that if you send your twin on a fast round trip rocket flight he/she will return younger than you. See the reference (Frauenfelder, 1962, page 63) for more details.

The strategy of this experiment is as follows:

1) Operate the spectrometer at very high dispersion and calibrate it by measuring the separation between the two central peaks of the ^{57}Fe spectrum;

2) Measure the fractional shift position $\Delta E/E$ of the single peak of stainless steel between room temperature T and $T+\Delta T$;

3) Compare the result with the theory of Josephson.

To measure the temperature effect reduce the velocity amplitude of the Mössbauer drive so that the two central components of the Zeeman pattern are widely separated, say by 400 channels, i.e. increase the dispersion of the spectrometer so that the small effect of temperature will be able to cause a shift of several channels in the centroids of the Zeeman lines. Calibrate the velocity scale by recording the locations of the central two peaks of the ^{57}Fe spectrum. Place the aluminum-block oven with the Mylar windows, containing the thin stainless steel and attached heater and thermocouple, in position between source and counter. Accumulate a spectrum with sufficient counts so that the positions of the peaks of the absorption line can be determined with an uncertainty no greater than ±1 channel.. Adjust the temperature control to ~120°C and turn on the heater. When the temperature has stabilized record a high-temperature spectrum. Repeat cold and hot measurements several times to reduce and evaluate your random error. Determine the temperature coefficient from your data, i.e. the fractional change in the peak energies per degree centigrade, and compare your results with the theoretical prediction (see the discussion in Frauenfelder, 1962, page 63).

c. Quadrupole splitting and isomer shifts in Fe^{++} and Fe^{+++} ions.

Measure the absorption spectra in samples of $FeSO_4.7H_2O$ and $Fe_2(SO_4)_3$ and determine the quadrupole splittings (if any) and the isomer shifts. Accumulations of 30 to 60 minutes should be sufficient to show the absorption spectra and permit accurate measurement of the splittings. See DeBenedetti (1960) for a discussion of the implications of such measurements.

d. Combined Zeeman and quadrupole effects in Fe_2O_3.

Measure the absorption spectrum of an isotope-enriched sample of red (ferrous) iron oxide, Fe_2O_3. (Note that the red oxide, otherwise known as rust, is not ferromagnetic, i.e. it is not attracted by a magnet.) Allowing for the combined effects of Zeeman and quadrupole splitting, and using the value for the magnetic moment of the first excited state obtained above, derive the strength of the magnetic field at the iron nuclei in red oxide, and the magnitude of the product of the quadrupole moment and the electric field gradient.

e. The absorption spectrum of magnetite (Fe_3O_4; the black magnetic oxide of iron).

Try to figure out what is going on.

The available samples of magnetite require long exposures because they have only the natural abundance of ~2%. The Mössbauer spectrum of magnetite has provided important clues to the structure of this peculiarly complex substance. You will probably need to dig into the literature for help in the interpretation of the spectrum. There is an extensive series of reviews on Mössbauer spectroscopy in the Science Library. Incidentally, the black sand that you may have seen on ocean beaches is magnetite.

f.The charge of the photon.

Suppose that the photon, instead of being neutral, had a very small electric charge. Since a charge q, moving through an electrostatic potential V, suffers an energy change $\Delta E = qV$, one could use the Mössbauer effect to measure this charge by applying a DC voltage between a source of gamma-rays and an absorber. Estimate the upper bound you could place on the magnitude of the charge on the photon in such a measurement?

g. Other iron-bearing materials, like rust, cast iron filings, spring steel, medicinal iron pills, black sand.

REFERENCES

Boyle and Hall, *Reports on Progress in Physics*, **XXV** (London 1962), p. 441.

S. DeBenedetti, "The Mössbauer Effect", *Sci. Amer.* (April, 1960).

H. Frauenfelder, *The Mössbauer Effect* (Benjamin: New York 1962).

S. Gasiorowicz, *Quantum Physics* (Wiley: New York 1974).

*S. S. Hanna, J. Heberle, C. Littlejohn, G. J. Perlow, R. S. Preston, and D. H. Vincent, *Phys. Rev. Letters.*, **4**, 177 (1960).

*O. C. Kistner, A. N. Sunyar, "Evidence for quadrupole Interactions of Fe^{57m} and Influences of Chemical Binding on Nuclear Gamma-Ray Energy", *Phys. Rev. Letters*, **4**, 412 (1960).

A. C. Melissinos, *Experiments in Modern Physics* (Academic Press: Orlando 1966).

"Mössbauer Effect -- Selected Reprints" (American Institute of Physics: New York 1963).
S. L. Ruby, L. M. Epstein, and K. H. Sun, *Rev. Sci. Instr.*, **31**, 580 (1960).

* reprinted in Frauenfelder (1962).